



Digital element approach for simulating impact and penetration of textiles

Youqi Wang^{a,*}, Yuyang Miao^a, Daniel Swenson^a, Bryan A. Cheeseman^b, Chian-Feng Yen^b, Bruce LaMattina^c

^a Department of Mechanical and Nuclear Engineering, Kansas State University, Manhattan, Kansas 66506, USA

^b US Army Research Laboratory, Aberdeen Proving Ground, MD 21005, USA

^c US Army Research Office, Durham, NC 27703, USA

ARTICLE INFO

Article history:

Received 2 March 2009

Received in revised form

25 September 2009

Accepted 23 October 2009

Available online 1 November 2009

Keywords:

High speed penetration

Digital element simulation

Ballistic resistance

Fabrics

Body armor

ABSTRACT

A micro-scale computational tool, based upon an explicit digital element method (DEM), has been developed for numerical simulation of ballistic impact and penetration of textile fabrics. In this approach, each yarn is digitized as an assembly of digital fibers. Each digital fiber is further digitized into a short digital rod element chain connected by frictionless pins (nodes). A search is conducted to find contacts between adjacent digital fibers. If a contact is detected, compressive and frictional forces between fibers will be determined, based upon contact stiffness and friction coefficient. Nodal forces are calculated for each time step. Nodal displacements are determined using an explicit procedure. Because the digital element approach operates on a sub-yarn micro-scale, one can determine textile penetration resistance based upon sub-yarn scale properties, such as inter-fiber compression, friction, and fiber strength. Research presented in this paper includes three parts. First, the explicit digital element algorithm used in dynamic simulation is explained. Second, the approach is used to generate 2-D woven fabric micro-geometries and to simulate ballistic penetration processes. Third, numerical results are compared to high resolution experimental impact and ballistic test data.

© 2009 Elsevier Ltd. All rights reserved.

1. Introduction

Compliant textile garments developed for protection have been produced for thousands of years – from layers of linen utilized by the ancient Greeks through layers of silk worn by medieval Japanese samurai. In the late 19th century the U.S. military also used silk body armor. During World War II, the “flak jacket”, constructed of ballistic nylon, was developed. However, none of these early protective textiles could resist a high velocity bullet. In the late 1960s, Du Pont invented Kevlar, an aramid material, the first bullet-resistant fiber. This ushered in a new era of textile armor that continues to progress toward more efficient systems, offering exceptional protection against bullet penetration. While Kevlar was the first ballistic material from which modern body armor could be constructed, there are presently several other fiber types used in bullet-resistant armor, such as Twaron[®], Dyneema[®], Spectra[®], and Zylon[®].

Fabric penetration resistance is determined not only by fiber physical properties, such as strength, modulus, density, viscosity and thermal properties, but also by fabric structural geometry. How

a ballistic textile is manufactured and its resulting configuration directly influences its behaviours.

Since the 1960s, numerous numerical methods for simulating textile penetration have been developed. However, the design and development of textile armor systems have been driven primarily by experiments and experience. Numerical models typically have not been used to predict design of armor systems. Rather, they have been used to provide insight into the relative importance of specific material parameters that influence performance. Although textile performance is directly related to the manufacturing process and its resulting fabric architecture, most of the important details related to fabric micro-structure and filament-level physics, such as yarn denier, end count, tow structures, filament spatial paths, and fiber-to-fiber interaction were not accurately modeled in previous numerical techniques. As a result, these models could not establish a quantitative relation among material properties, manufacturing process, fabric micro-geometry, and ballistic performance.

In order to improve numerical model accuracy, a sub-yarn micro-scale explicit digital element algorithm has been developed for numerical simulation of the ballistic impact and the penetration of textile fabrics. The digital element method (DEM) was originally developed to simulate textile processes and to determine textile fabric micro-geometries [1–5]. In this model, a yarn is discretized as an assembly of digital fibers. A digital fiber is modeled as a rod

* Corresponding author. Tel: +1 785 532 7181; fax: +1 785 532 7057.
E-mail address: wang@mne.ksu.edu (Y. Wang).

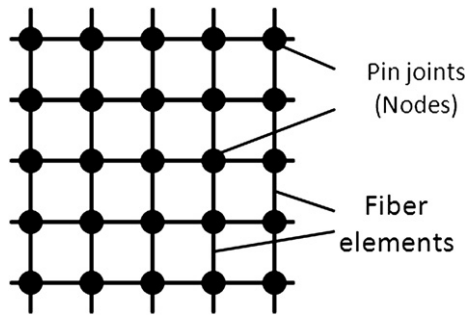


Fig. 1. Roylance model.

element chain. When distance between two digital fibers is smaller than fiber diameter, a contact element between them is established. The textile process is modeled as a quasi-static non-continuum mechanics problem with boundary conditions. In this paper, a computer tool, based upon an explicit digital element algorithm, is developed for fabric dynamic analysis. It is used to simulate fabric response to impact and ballistic penetration. Numerical results are compared to results from fabric impact and ballistic tests. Comparisons indicate good agreement between digital element prediction and experimental results.

2. Background

Textiles are comprised of many filaments, arranged in bundles, called a yarn. Yarns are organized in tows. The tows are assembled into fabric in specific patterns through weaving or braiding processes. The level of geometric representation of the numerical model dictates the resolution of the numerical results. If a fabric is considered as a continuum, details of tow-to-tow interaction and projectile-to-tow interaction cannot be modeled. As a result, the effect of fabric patterns on ballistic resistance cannot be analyzed. If a tow or a yarn is represented as a continuum, details of filament-

to-filament interaction and projectile-to-filament interaction cannot be modeled. As a result, the effect of tow or yarn micro-geometry on the ballistic resistance cannot be analyzed.

With the advent of modern ballistic fibers, scientists began to develop computational tools to analyze the penetration resistance performance of textile fabrics made from these fibers. Generally speaking, the research can be divided into two approaches. In one approach, fabrics are modeled as a homogenous continuum. The second approach uses a more detailed geometric representation in which tows (or yarns) are represented as a homogenous continuum. A fabric is then an assembly of tows (or yarns) with a specific pattern.

Numerous models using the homogeneous continuum fabric assumption have been developed since the 1970s. Some representative models include: a homogeneous and isotropic plate which deforms into a straight sided conical shell when impacted by a projectile (Vinson and Zukas [6], 1975, and Taylor and Vinson [7], 1990); a two dimensional isotropic membrane (Phoenix and Porwal [8], 2003); an anisotropic membrane (Simons et al. [9], 2001); use of a system of linear springs to represent continuum behaviour (Walker [10], 1999); and a visco-elastic continuum with rate dependent failure (Lim et al. [11], 2002). While all of these efforts report reasonable success when compared with experiment results, these approaches are inherently limited as they cannot account for important details such as yarn-to-yarn and projectile-to-yarn interaction, which has been shown to influence the textile ballistic performance (Briscoe and Motamedi [12], 1992, and Bhatnagar [13], 2006). Recent efforts (King et al. [14], 2005, and Boljen and Hiermaier [15], 2006) have resulted in multi-scale formulations that account for the micro-structural aspects of a textile within a membrane formulation.

A more detailed geometric approach started with the pioneering work of Roylance and his coworkers [16]. In their model, a 2-D woven fabric is simplified as a 2-D fiber element network, as shown in Fig. 1. Fiber elements are pin-jointed at crossover points. Therefore, it is commonly called a pin-joint model. Longitudinal properties of fiber elements are defined by fiber/yarn modulus and

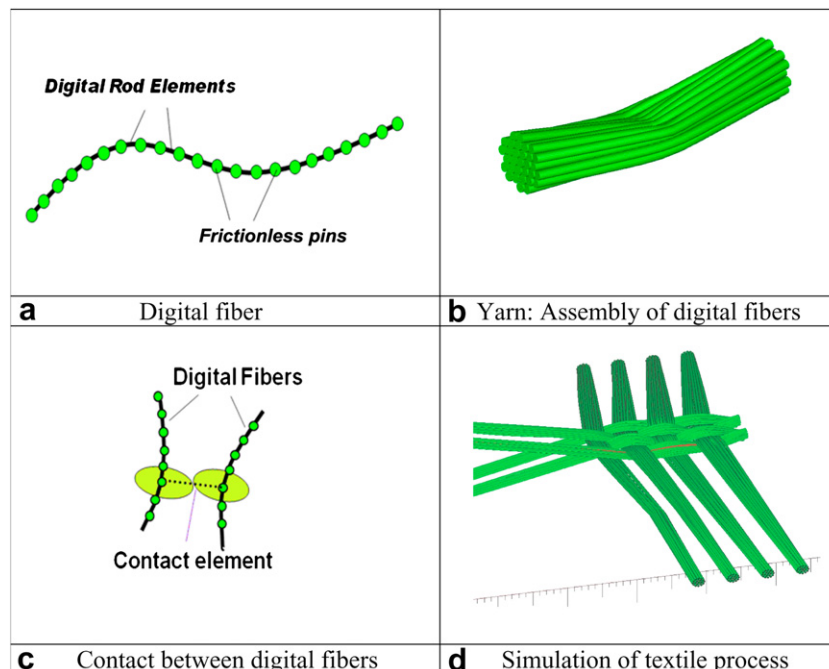


Fig. 2. Concept of digital element simulation [3–5].

strength. The Roylance model supplies insight into relations between yarn properties and penetration resistance. It has been employed and extended by a number of other researchers to include additional physical properties: yarn slippage (Roylance [17], 1995), projectile geometries and edge conditions (Cunniff [18], 1992), nonlinear visco-elastic effects (Roylance and Wang [19], 1981), multiple plies (Ting et al. [20], 1993), yarn crimp (Shim et al. [21], 1995), and slip at yarn crossover points (Ting et al. [22], 1998). Yet, the representation of the textile with this approach does not reflect the complex fabric topology and yarn micro-geometry. As noted by Roylance [16], 1973, “the ballistic response of the textile structure depends on the response of the fiber with which it is woven as well as the structural geometry itself.”

As detailed above, numerical simulations of textile protection systems are not new, but the resolution that can be attained has been greatly enhanced as computer power has progressed. Cuttiff [18], 1992, stated that the cost of performing numerical simulations of 50 layers of fabric modeled at the detail of the yarn crossover would be far in excess of building and testing the system. However, since that time, computer power has increased dramatically. Numerical simulations of textiles comprised of discrete yarns and multiple layers have become possible. Shockey et al., (Shockey, Giovanola, Simons, Erlich, Kolpp and Skaggs [23], 1997), were among the first researchers to perform finite element simulations of impact into a fabric with each individual yarn represented with solid elements. These researchers analyzed the impact of a turbine fan blade, traveling approximately 80 m/s, on woven containment shrouds. Using this same level of resolution, Duan et al. (Duan, Keefe, Bogetti, Cheeseman and Power [24,25], 2005 and 2006) investigated the impact of steel spheres and right circular cylinders of a single-ply of Kevlar. Although the development of these detailed finite element meshes is labor intensive, this has not dissuaded a number of other researchers from advancing these detailed simulations and incorporating refinements such as multiple layers. Recent efforts were made by Gu [26], 2004, by Scott and Yen [27], 2005, by Boljen and Hiermaier [15], 2006 and by Zohdi and Powell [28], 2006. Boljen and Hiermaier generated FEM model for different weaves, and Zohdi and Powell modeled fabrics on a filament scale.

In this paper, a unique approach, “a digital element approach” [1–5], is employed to simulate the penetration process. Fig. 2 illustrates this approach. It includes three key concepts: digital fibers, yarn assembly and contact between digital fibers. Refer to Fig. 2-a. A digital fiber is a physical representation of a fiber. It is composed of many rod elements which are connected by frictionless pins. As the element length approaches zero, the digital fiber

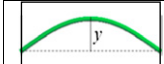
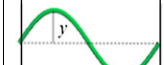

	Initial Deflection $y = 1\text{mm}$		Initial Deflection $y = 0.1\text{ mm}$	
	Numerical	Analytical	Numerical	Analytical
	0.0002823s	0.00028206s	0.00028205s	0.00028206s
	0.00014152s	0.00014103s	0.00014103s	0.00014103s
	0.000094772s	0.000094020s	0.000094025s	0.000094020s

Fig. 4. Comparison of vibration periods.

becomes fully flexible and behaves like an actual fiber. Digital fibers are organized into bundles, forming a yarn. Fig. 2-b shows a yarn deformed due to a transverse load. Contact between digital fibers is modeled by searching for contact with adjacent fibers. If contact is detected, a contact element is inserted, as shown in Fig. 2-c. Both compressive and friction forces between fibers are calculated. In previous research [1–5], Wang and her coworkers developed a computer tool to simulate various textile processes based upon a quasi-static numerical algorithm. Fig. 2-d shows a small 2-D woven fabric generated by the computer tool.

With the explicit digital element approach, one can conduct a dynamic simulation at near filament-level resolution. The essential physics of the problem, such as fiber failure, fiber-to-fiber contact, and fiber-to-fiber friction, can therefore be modeled. The purpose of this research is to develop an explicit digital element computer tool with sufficient accuracy to predict textile fabric ballistic strength, so it could be used for ballistic fabric design.

The numerical procedure in the digital element analysis is similar to that in the finite element analysis. For this reason, it was called a FEM approach when initially published [1]. Later, it was renamed “digital element method” [2–5] because of a conceptual difference between them.

In a finite element analysis, a material domain is discretized into many elements. Each element preserves all the physical properties of the original material domain. The purpose of the discretization is to describe the displacement field and the stress field through element shape functions. When element size approaches zero, element shape functions are capable of collectively representing any arbitrary displacement field and stress field. If this occurs, the

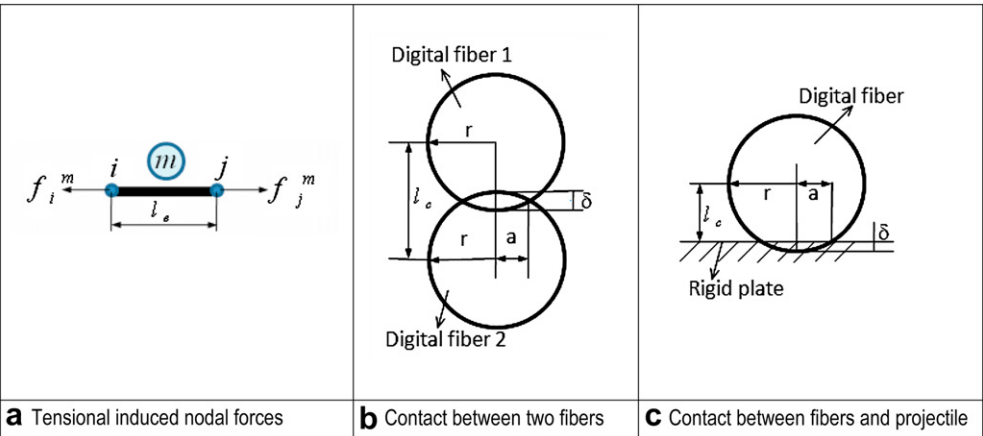


Fig. 3. Nodal force calculations.

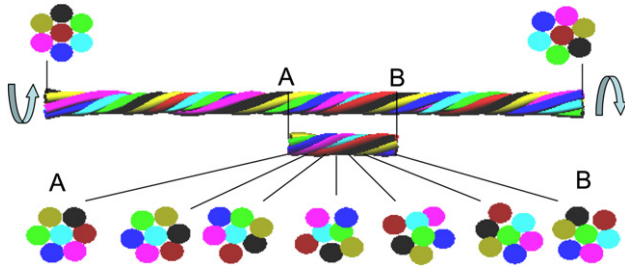


Fig. 5. Twisted yarn.

FEM results converge. The FEM discretization procedure is a mathematical discretization. Physical properties of a material domain remain unchanged before and after mesh generation.

In the digital element analysis, a digital fiber is discretized into many rod elements and a yarn is discretized into many digital fibers. The purpose of discretization is to change physical properties. Prior to discretization, the digital fiber is a rigid one-dimensional truss. Post discretization, it becomes a flexible one-dimensional body with fiber or yarn like properties. Prior to discretization, a yarn is a continuum body with a circular cross-section. Post discretization, a yarn is split into numerous digital fibers. Therefore, DEM discretization is a physical discretization: It is used to generate digital fibers and yarns with special properties. The convergence theory in FEM is no longer applicable.

In FEM analysis, one could achieve the same accuracy by choosing smaller elements with lower degree shape functions or by choosing larger elements with higher degree shape functions. In contrast, in digital element analysis, the accuracy of fabric physical properties is determined by element lengths and digital fiber diameters. Error induced by physical discretization cannot be reversed through a mathematical process, i.e. the use of high degree shape functions. The accuracy of a DEM analysis depends upon the discretization resolution.

3. Explicit digital element algorithm

3.1. Explicit algorithm

A central-difference explicit numerical algorithm is employed to minimize computer memory resource requirements [29]. Assume that i denotes the nodal number, m_i denotes the mass of node i , a_i denotes the acceleration of node i , v_i denotes the velocity of node i , Δt denotes the time step, and u_i denotes the displacement of node i , and n counts the step. The algorithm is divided into three steps as shown in the following equations:

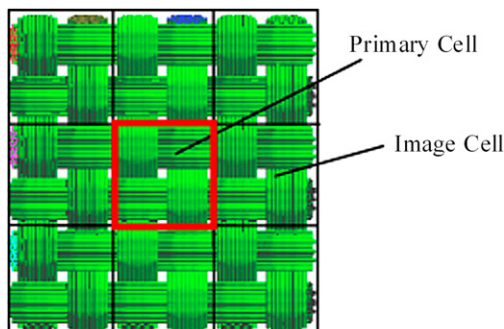


Fig. 6. Relaxation process with periodic boundary condition.

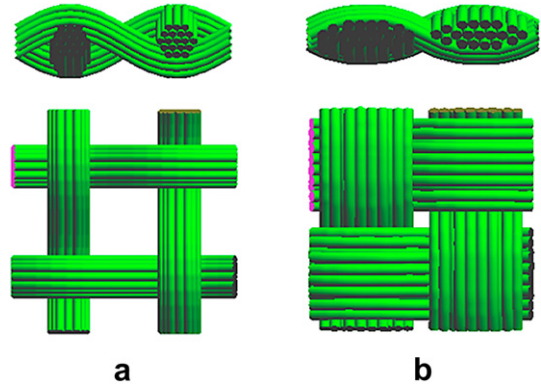


Fig. 7. Fabric micro-geometry generated using dynamic relaxation process. (a) Initial micro-geometry (b) Relaxed micro-geometry.

$$(\mathbf{a}_i)_n = \frac{(\mathbf{f}_i)_n}{m_i}$$

$$(\mathbf{v}_i)_{n+1/2} = (\mathbf{v}_i)_{n-1/2} + (\mathbf{a}_i)_n \Delta t \quad (1)$$

$$(\mathbf{u}_i)_{n+1} = (\mathbf{u}_i)_n + (\mathbf{v}_i)_{n+1/2} \Delta t$$

where \mathbf{f}_i represents the total resultant nodal force applied to node i , which is induced by fiber tension, fiber-to-fiber contact, fiber-to-fiber friction, fiber-to-bullet friction, and fiber-to-bullet contact.

3.2. Nodal force

3.2.1. Element tension induced nodal forces

As shown in Fig. 3-a, element m has two nodes: i and j . Element tension induces nodal forces at both nodes i and j as:

$$\mathbf{f}_i^m = -\frac{E_L A_e}{l_e} \Delta l_e, \quad \mathbf{f}_j^m = \frac{E_L A_e}{l_e} \Delta l_e \quad (2)$$

where E_L is the digital fiber modulus; A_e is the digital fiber cross-section area; l_e is the original element length, and Δl_e is the elongation of the digital element.

3.2.2. Fiber-to-fiber compression

When the distance of two nodes from adjacent fibers is smaller than the fiber diameter, contact is represented between the two nodes. The contact stiffness is calculated as:

$$k_n = \frac{E_T A_c}{l_c} \quad (3)$$

where E_T is the fiber transverse modulus; l_c is the contact distance, defined by distance between two nodes; and A_c is the contact area. The contact area calculation assumes that the two digital elements have parallel alignment. As shown in Fig. 3-b, the contact area is given by

$$A_c = 2al_e \quad (4)$$

where a can be calculated as:

Table 1

Properties of Kevlar KM2 fiber [32] and Spectra 900 fibers [33].

Properties	E_1 (GPa)	E_2 (GPa)	Strength (GPa)	ρ (kg/m ³)
Kevlar KM2	82.6	1.34	3.4	1440
Spectra 900	79	0.79	2.61	970

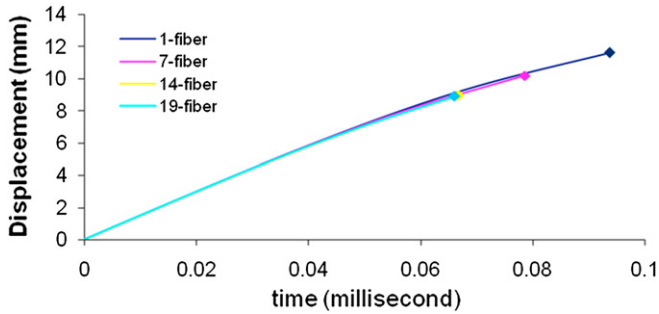


Fig. 8. Projectile displacement vs. time after striking.

$$a = \sqrt{R^2 - (R - \delta/2)^2} \approx \sqrt{R\delta} \quad (5)$$

The compressive force between two digital fibers is calculated as

$$F_n = \int_0^\delta k_n d\delta = \frac{4E_T l_e \sqrt{R}}{3l_c} \delta^{3/2} \quad (6)$$

3.2.3. Fiber-to-projectile compression

Because projectile diameter is much greater than fiber diameter and because projectile stiffness is much greater than fiber lateral stiffness, the projectile is assumed to act as a rigid plate, Fig. 3-c. A similar procedure used to calculate contact between fibers is used to calculate contact between fibers and projectile. Equation (6) is used to calculate compression force. However, the contact length l_c in equation (6) represents the distance between the node of the digital fiber and the surface of the projectile.

3.2.4. Fiber-to-fiber friction

When two nodes first contact, no relative sliding occurs. Friction force increment in subsequent steps is calculated as:

$$F_s = k_s u_s \quad (7)$$

where k_s is the friction stiffness and u_s is the relative tangential displacement after contact occurs. It is assumed that $k_s = \mu k_n$ where μ denotes the friction coefficient.

A Coulomb friction model is assumed. If the calculated friction force $|F_s| > \mu F_n$, sliding will occur and $|F_s| = \mu F_n$. Force direction is determined by relative tangential displacement in the previous time step.

3.2.5. Fiber-to-projectile friction

Fiber-to-projectile friction is calculated similarly. When a node that belongs to a digital fiber contacts the surface of the projectile, it sticks to the surface until $|F_s| > \mu F_n$. Friction force direction is determined by the relative tangential motion that occurred in the previous time step.

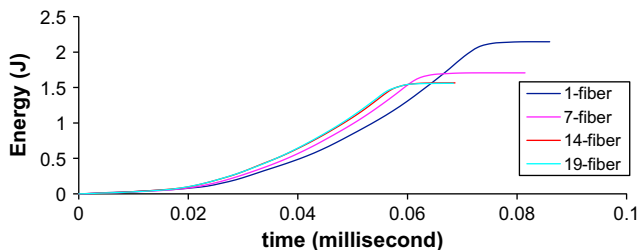


Fig. 9. Projectile energy loss vs. time after striking.

Table 2

Residual velocity of projectile (striking velocity: 100 m/s, fabric dimension: 33 mm × 33 mm).

Number of digital fibers per yarn	1 digital fiber	7 digital fibers	14 digital fibers	19 digital fibers
Residual velocity (m/s)	55.45	67	70.32	70.51

3.3. Element failure

Element strain and stress are calculated during each numerical simulation step. If element stress is greater than fiber strength, element failure occurs. Failed elements are removed from the system permanently.

3.4. Numerical examples

Two numerical examples are presented to verify accuracy and feasibility.

3.4.1. Example 1: Lateral string vibration

Lateral string vibration is simulated with string modulus 72.4 GPa, density 1440 kg/m³, and string diameter 1.2 mm (Fig. 4). String length is 100 mm. 100 digital elements are employed. An initial strain of 1% is assumed. The three initial mode shapes are shown on the left side of Fig. 4. Initial-lateral deflection magnitudes are assumed to be 0.1 mm or 1 mm, respectively. Vibration periods derived from the analytic free-string vibration solution [30] are compared to vibration periods obtained from the numerical solution.

When the initial deflection is 0.1 mm, differences between numerical solutions and analytical solutions are smaller than 0.01%. When the initial deflection equals 1 mm, differences between numerical solutions and analytical solutions range between 0.1% and 1%. The difference between a numerical result and an analytical result increases as initial-lateral deflection increases. This is due to the constant string tension assumption used in the analytic solution. This assumption is true only when the initial-lateral deflection approaches zero. The comparison validates the digital element approach for free-string vibration simulation.

3.4.2. Example 2: Yarn twisting process

The explicit code is also employed to simulate a twist process (Fig. 5). In this model, a yarn consists of seven fibers. During the twisting process, relative positions of the seven fibers within the cross-section constantly change due to tension differences. The spatial paths of fibers in the outer region are longer than the spatial path of the center fiber. This causes tensile force to develop in the outer region fibers and compressive force to develop in the center fiber. As such, the center fiber buckles and migrates to an outer region due to transverse compressive force applied by fibers in the outer paths. Each fiber originally located in an outer path migrates in turn into the center as the center fiber migrates into an outer path.

Fig. 5 shows details of fiber migration for the segment between A and B. The light blue fiber, originally located in the

Table 3

Residual velocity of projectile (striking velocity: 150 m/s, fabric dimension: 50 mm × 100 mm).

Number of digital fibers per yarn	1 digital fiber	7 digital fibers	14 digital fibers	19 digital fibers
Residual velocity (m/s)	83.2	99.26	109.35	109.61



Fig. 10. Out-plane deflection of impacted fabrics from digital element simulation.

center, gradually migrates to an outer position; the green fiber, originally located in the outer position, gradually migrates to the center position. In addition, the twisted yarn cross-section does not retain a circular shape due to the unstable fiber migration.

There is no analytical solution for the problem. However, the phenomenon captured in the numerical simulation is similar to observations described by Hearle [31].

4. Generation of micro-geometry of textile fabrics

The first step toward ballistic penetration simulation is to generate a textile fabric with a detailed micro-geometry. It is not sufficient to just define the woven topology and directly proceed to fabric analysis. Instead, it is necessary to use the topology and a relaxation process to obtain a state that represents an as-woven fabric, with yarns compressed due to contact. This deformed state can then be used as the initial state for a penetration analysis.

To reach the deformed state, we use a unit-cell model with a periodic boundary condition. An explicit dynamic relaxation procedure is adopted. The process is shown in Figs. 6 and 7. Fig. 6 shows a fabric with nine unit cells. The unit cell in the center is called the primary cell; the other eight are images of the primary cell. The initial micro-geometry of the primary cell, i.e., the first guess of the micro-geometry, is defined based upon the weaving pattern, as shown in Fig. 7-a. The relaxation process is divided into two stages. During the first stage, a yarn tension of 0–1 N is assumed. During each relaxation step, element stresses within each yarn are calculated. The average of these element stresses is defined as the yarn stress. The yarn tension can be then derived. If the calculated yarn tension differs from the assumed yarn tension, a pre-tension term is added to every element of the yarn in order to adjust the yarn tension to the assumed value. Nodal forces and nodal displacements in the primary cell are then calculated. Nodal displacements inside the primary cell are mapped to the eight image cells. To dampen fabric oscillation, approximately 20%–50% of kinetic energy is removed during each time step. During the second stage, the yarn tension is assumed to be a near-zero positive value. Relaxation continues until all nodal forces approach zero. This provides a unit cell that represents the as-woven fabric, as shown in Fig. 7-b. This relaxed unit cell is then replicated to form the model of the woven fabric used for penetration analysis.

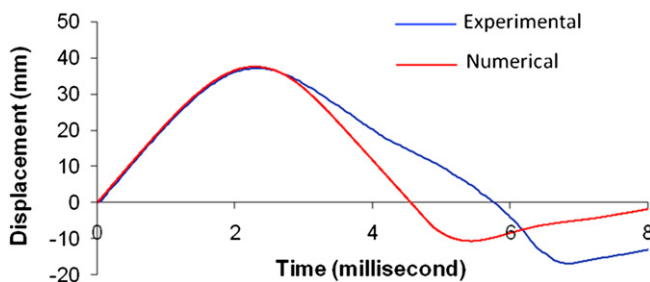


Fig. 11. Comparison of fabric deflection in impact area: circular fixture.

5. Simulation of ballistic penetrations

5.1. Convergence of digital element simulation

The explicit digital element approach is then used to simulate ballistic penetration through a small fabric. In an actual fabric, each yarn contains hundreds of fibers. In the numerical simulation, it is neither possible, nor necessary, to model the yarn as an assembly of hundreds of fibers. In order to check the convergence of the digital element approach, ballistic penetration processes through fabrics were simulated with yarns modeled as assemblies of 1 digital fiber, 7 digital fibers, 14 digital fibers and 19 digital fibers. In all the examples shown in this subsection, the digital element length is equal to the element radius. As a yarn is split into more digital fibers, the fiber radius becomes smaller and the element length becomes smaller. As such, more accurate results are expected from the numerical simulation.

The fabric used for the convergence analysis is Kevlar KM2 plain weave, 34×34 yarns per inch. Fabric density is 180 g/m^2 . In the first example, fabric dimension is 33 mm by 33 mm. Fixed boundary conditions are employed on all four sides. Fiber properties are listed in Table 1, which are taken from ref. [32,33]. The bullet is a spherical projectile with a diameter of 8 mm and a mass of 2.091 g. It strikes the fabric with a velocity of 100 m/s. The fabric fails and the projectile penetrates through the fabric with a residual velocity.

Fig. 8 shows projectile displacement vs. time curves. There are four curves, which are derived from the 1-, 7-, 14-, and 19-digital fiber yarn models, respectively. The diamond shows locations where the projectile penetrates fabric. One can see that the four displacement curves almost overlap before penetrations occur. However, penetration occurs at different times.

Fig. 9 shows the four projectile energy loss curves. Energy loss predicted by the single digital fiber yarn model is higher than that predicted by the 7-digital fiber yarn model. Energy loss derived from the 7-digital fiber yarn model is slightly higher than that derived from the 14-digital fiber yarn model. The energy loss derived from the 14-digital fiber yarn model is almost the same as that derived from the 19-digital fiber yarn model. Numerical results converge when more and more digital fibers are used to represent a yarn.

Table 2 is the comparison of the residual projectile velocities after penetration. A similar convergence pattern is shown. The residual

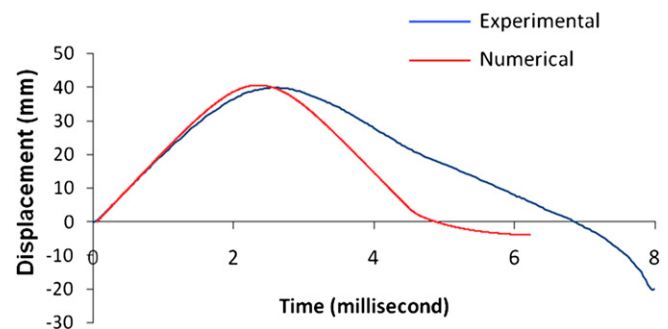


Fig. 12. Comparison of fabric deflection in impact area: square fixture.

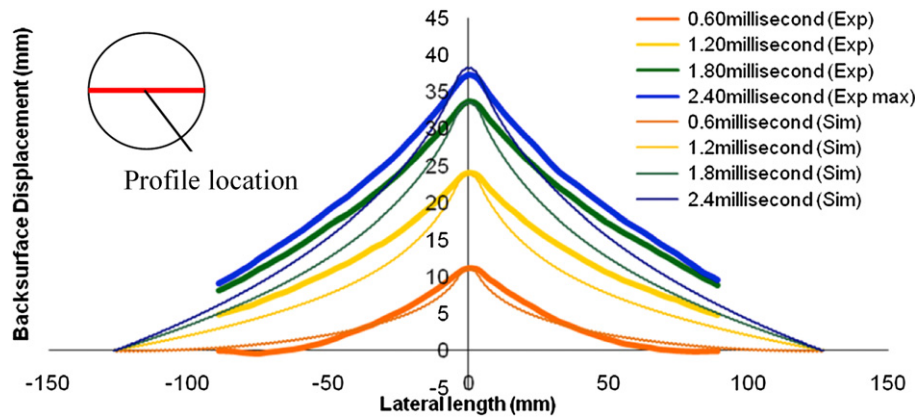


Fig. 13. Comparison of displacement profile: circular fixture.

velocity derived from the 14 digital fiber yarn model is almost the same as that derived from the 19-digital fiber yarn model.

A similar convergence study used the same fabric with a larger dimension and higher striking velocity. The fabric dimension was 50 mm by 100 mm and the striking velocity was 150 m/s. A similar conclusion was reached: the results derived from the 14 digital fiber yarn model are almost the same as that derived from the 19-digital fiber yarn model. Results are convergent in a similar pattern. Table 3 shows the comparison of residual velocities.

5.2. Comparison between numerical results and high resolution experimental results

A series of impact experiments were conducted by Weerasooriya et al. [34] on a single-ply Kevlar KM2 woven fabric (Kevlar Style 706 fabric produced by Hexcel corporation). The dimension of each fabric was 406.4 mm × 406.4 mm, which was clamped in a fixture with either a 254 mm × 254 mm square opening or a 254 mm diameter circular opening. The fabric was impacted at the center of the opening by a hemispherical-nosed steel projectile. Projectile nose diameter was 13 mm, projectile mass 104 g and striking velocity 22 m/s. High speed digital image correlation (DIC) techniques were utilized to measure fabric full-field out-of-plane deflection. In these experiments, there was no penetration of the fabric, instead the projectile rebounded.

The impact process was simulated using the digital element approach. Kevlar KM2 fiber properties [32] listed in Table 1 were

used in numerical simulations. Fixed boundary conditions were employed along the edge of fixture openings. Fig. 10 shows out-plane deflections induced by impact on fabrics with circular and square boundary conditions, respectively. Fabric deflections in the impact area, which were derived from digital element simulation, were then compared to measured fabric deflections, as shown in Figs. 11 and 12. Two curves are shown in each of these two figures: blue and red. The blue curves are fabric deflections derived from experimental measurement. The red curves are fabric deflections at the impact area derived from numerical simulation. Good correlation is noted between the measured and calculated deflection histories in the impact areas until the fabric deflection reaches the maximum. At that point, the fabric springs back in the opposite direction. Deflection decreases and the simulation curves begin to separate from measured curves.

Figs. 13 and 14 compare the displacement profiles obtained from numerical simulations and experiments. Profile locations are shown in the upper-left corners of these figures. Four experimental curves and four numerical curves are shown in each figure. Thicker curves were derived from experimental measurements, which represent fabric profile at 0.6 ms, 1.2 ms, 1.8 ms and 2.4 ms after the projectile contacts the fabric. Thinner curves were derived from numerical simulations. For both cases, calculated deflections in fabric centers, i.e., impact areas, match well with measured deflections. However, discrepancies are noted when comparing profile shapes.

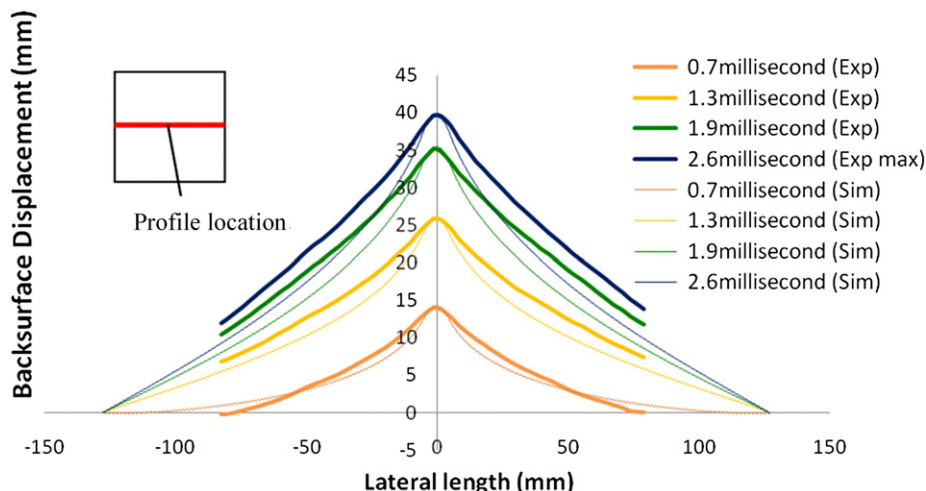


Fig. 14. Comparison of displacement profile: square fixture.

Table 4

Comparison between numerical and experimental results.

Fabric	Layers	Obliquity	Numerical results			V_{50} (m/s) experimental results
			Striking velocity	Penetration status	Estimation of V_{50} (m/s)	
Kevlar 706	1	0°	106.3 m/s	Stopped	106.3–111.3	106.3
Kevlar 706	1	45°	111.3 m/s	Penetrated	97.5–102.5	97.5
			97.5 m/s	Stopped		
Kevlar 706	2	0°	102.5 m/s	Penetrated	162.3–172.3	162.3
			162.3 m/s	Stopped		
Kevlar 706	2	45°	172.3 m/s	Penetrated	155.8–165.8	155.8
			155.8 m/s	Stopped		
Spectra 900	1	0°	165.8 m/s	Penetrated	193.6–213.6	193.6
			193.6 m/s	Stopped		
Spectra 900	1	45°	213.6 m/s	Penetrated	152.5–167.5	152.5
			152.5 m/s	Stopped		
Spectra 900	2	0°	167.5 m/s	Penetrated	226.5–250.5	226.5
			226.5 m/s	Stopped		
Spectra 900	2	45°	250.5 m/s	Penetrated	193.9–225	193.9
			193.9 m/s	Stopped		
			225 m/s	Penetrated		

Overall agreement between simulation and experimental results is good. Noted discrepancies may be due to the following three reasons:

- Digital fiber is more flexible than actual fiber. Fiber bending stiffness is neglected in the numerical model. Actual fibers and yarns have a small bending stiffness. Neglecting bending stiffness may slightly affect the fabric deflection profile.
- Air damping effect was not considered in numerical simulation.
- Fiber has nonlinear elasto-plastic transverse stress–strain relations [32]. Energy loss due to lateral fiber-to-fiber compression is not considered in the numerical simulation.

5.3. Comparison between numerical results and ballistic impact results

The digital element approach was also used to predict V_{50} of ballistic fabrics. Results were compared to ballistic tests conducted by Schiffman and Wetzel at ARL [35]. Two types of fabrics were used in this comparison:

- Hexcel Schwebel Style 706: Kevlar KM2 fibers, 34×34 yarns per inch, plain weave, 180 g/m^2
- Hexcel Schwebel Style 904: Spectra 900, 34×34 yarns per inch, plain weave, 203 g/m^2

One or two layer fabrics were used in the ballistic tests. Fabrics were clamped in a frame with a $50 \text{ mm} \times 100 \text{ mm}$ opening and the spherical projectiles impacted at angles of 0° and 45° . In the numerical simulations, properties of Kevlar KM2 fibers and Spectra 900 were taken from ref. [32] and [33], respectively. They are listed in Table 1. No data was found on the transverse moduli of spectra 900. They were assumed to be one percent of the longitudinal moduli. The fiber-to-fiber friction coefficients and fiber-to-projectile friction coefficients were also unknown. They were assumed to be 0.2.

Numerical and experimental results are compared in Table 4. There are three columns under numerical results in Table 4. The first is striking velocity, the second penetration status. They are determined in the following way.

After a projectile strikes a fabric, there are three possibilities: 1) the projectile has a positive residual velocity after penetrating through the fabric, 2) the projectile stops and the fabric fails, so the residual velocity is zero, and 3) the projectile is stopped by the

fabric without significant damage, so the projectile springs back and the residual velocity is negative. If the residual velocity is positive, the penetration status is considered as “Penetrated”. If the residual velocity is zero or negative, the penetration status is considered as “Stopped”.

The third column is an estimation of V_{50} , which is based upon the penetration status in accordance with two numerical results. For example, for Kevlar 706, the penetration status is “stopped” when striking velocity is 106.3 m/s and “penetrated” when striking velocity is 111.3 m/s. The estimation of V_{50} is thus between these two striking velocities, i.e., 106.3–113.3 m/s.

For Kevlar KM2 fabrics, numerical results match experimental results very well. For Spectra 900 fabrics, numerical results were 5–10% higher than experimental results. Possible reasons for the discrepancy could be inaccuracies in the assumed fiber transverse moduli and friction coefficients. Generally speaking, the comparison shows the digital element approach is valid for the determination of ballistic penetration strength of single layer fabrics against a low speed projectile (100–200 m/s).

6. Conclusions

An explicit digital element algorithm has been developed to simulate ballistic penetration processes with near filament-level resolution. The following conclusions can be reached:

- Two numerical examples are presented to demonstrate the effectiveness of the approach. In the first example, a free-string vibration is simulated. Numerical results match analytical results. In the second example, a yarn twisting process is simulated. Numerical results successfully replicate observed fiber migration within the yarn cross-section.
- A dynamic relaxation algorithm with periodic boundary conditions is developed to generate unit-cell micro-geometries of textile fabrics. It is more efficient than previous step-by-step textile process simulation.
- The explicit digital element approach is then used to simulate ballistic penetration. In order to check the convergence of the numerical process, ballistic penetration through fabrics was simulated with yarns modeled as assemblies of 1, 7, 14 and 19-digital fibers. Numerical results converge with the increase of the digital fiber number in each yarn.
- Limited comparisons between results derived from numerical simulations and results derived from experiments were

conducted. Current results indicate good agreement. Further validation is required.

5. The DEM enables examination of the effects of micro-scale variables, such as fiber failure, fiber-to-fiber friction and fiber-to-fiber compression on fabric properties. More research will be conducted to link the filament-level properties to fabric strength.

Acknowledgements

The authors would like to acknowledge the Army Research Laboratory and Army Research Office for their financial support.

References

- [1] Wang Y, Sun X. Determining the geometry of textile performs using finite element analysis. In: Proceedings of the American society for composites, 15th ASC Technical Conference on Composite Materials, September 24–27, College Station, TX, vol. 9; 2000. p. 25–7.
- [2] Sun X, Wang Y. Geometry of 3-D Braiding rectangular perform with axial yarns. In: Proceedings of the 46th international SAMPE symposium, Long Beach Convention Center, CA, May 7–9, vol. 46; 2001. p. 2455–64.
- [3] Wang Y, Sun X. Digital element simulation of textile processes. *Journal of Composites Science and Technology* 2001;63:311–9.
- [4] Zhou G, Sun X, Wang Y. Multi-chain digital analysis in textile mechanics. *Journal of Composites Science and Technology* 2003;64:239–44.
- [5] Miao Y, Zhou E, Wang Y, Cheeseman B. Mechanics of textile composites: micro-geometry. *Journal of Composites Science and Technology* 2008. Vol. 68, No. 7–8, June, p. 1671–1678.
- [6] Vinson JR, Zukas JA. On the ballistic impact of textile body armor. *Transactions of the ASME Journal of Applied Mechanics* 1975;42:263–8.
- [7] Taylor Jr WA, Vinson JA. Modelling ballistic impact into flexible materials. *AIAA Journal* 1990;28:2098–103.
- [8] Phoenix SL, Porwal PK. A new membrane model for the ballistic impact response and V50 performance of multi-ply fibrous systems. *International Journal of Solids and Structures* 2003;40:6723–65.
- [9] Simons JW, Erlich DC, Shockey DA. Finite element design model for ballistic response of woven fabrics. In: Proceedings of 19th international symposium on ballistics, May 7–11, Interlaken, Switzerland 2001. p. 1415–22.
- [10] Walker JM. Constitutive model for fabrics with explicit static solution and ballistic limit. In: Proceedings of the 18th international symposium on ballistics, San Antonio, TX, Nov. 15–19, 1999, p. 1231–1238.
- [11] Lim CT, Shim VPW, Ng YH. Finite element modeling of the ballistic impact of fabric armor. *International Journal of Impact Engineering* 2002;28:13–31.
- [12] Briscoe BJ, Motamedi F. The ballistic impact characteristics of Aramid Fabrics – the influence of interface friction. *Wear* 1992;158:229–47.
- [13] Bhatnagar A. Bullets, fragments and bullet deformation. In: Bhatnagar A, editor. *Lightweight ballistic composites*. New York: CRC Press; 2006. p. 29–71.
- [14] King MJ, Jearanaisilawong P, Socrate S. A continuum constitutive model for the mechanical behavior of woven fabrics. *International Journal of Solids and Structures* 2005;42:3867–96.
- [15] Boljen M, Hiermaier S. Modelling of woven fabrics used as lightweight armor with respect to varying weave styles and interplay friction. In: US–German land combat lethality and survivability workshop; 2006.
- [16] Roylance D, Wilde A, Tocci G. Ballistic impact of textile structures. *Textile Research Journal* 1973;43:34–41.
- [17] Roylance D, Hammes P, Ting J, Chi H, Scott B. Numerical modeling of fabric impact, in high strain rate effects on polymer, metal and ceramic matrix composites and other advanced materials. In: Proceedings of the ASME international mechanical engineering congress and exposition, San Francisco, Oct. 1995., V. 48, p. 155–160.
- [18] Cunniff PM. An analysis of the system effects in woven fabrics under ballistic impact. *Textile Research Journal* 1992;62:495–509.
- [19] Roylance D, Wang SS. Influence of fiber material properties on ballistic penetration of textile panels. *Fiber Science and Technology* 1981;14: 183–90.
- [20] Ting J, Roylance D, Chi H, Chitrangad B. Numerical Modeling of Fabric Panel Response to Ballistic Impact. SAMPE proceedings, Philadelphia, PA; October 1993., p. 384–392.
- [21] Shim VPW, Tan VBC, Tay TE. Modelling deformation and damage characteristics of woven fabric under small projectile impact. *International Journal of Impact Engineering* 1995;16:585–605.
- [22] Ting C, Ting J, Cunniff P, Roylance D. Numerical characterization of the effects of transverse yarn interaction on textile ballistic response. In: 30th International SAMPE technical conference, October 20–24; 1998. p. 57–67.
- [23] Shockey DA, Giovanola JH, Simons JW, Erlich DC, Kolpp RW, Skaggs SR. Advanced armor technology: application potential for engine fragment barrier for commercial aircraft. U.S. Department of Transport; 1997. Federal Aviation Administration Report, DOT/FAA/AR97-53.
- [24] Duan Y, Keefe M, Bogetti TA, Cheeseman BA. Modeling friction effects on the ballistic impact behavior of single-ply high-strength fabric. *International Journal of Impact Engineering* 2005;31:996–1012.
- [25] Duan Y, Keefe M, Bogetti TA, Cheeseman BA, Powers B. A numerical investigation of the influence of friction on energy absorption by high-strength fabric subjected to ballistic impact. *International Journal of Impact Engineering* 2006;32:1299–312.
- [26] Gu B. Ballistic penetration of conically cylindrical steel projectiles into plain-woven fabric target – a finite element simulation. *Journal of Composite Materials* 2004;38:2049–74.
- [27] Scott BR, Yen CF. Analytic design trends in fabric armor. In: Proceedings of the 22nd international ballistics symposium; 2005. p. 752–60.
- [28] Zohdi TI, Powell D. Multiscale construction and large scale simulation of structural fabric undergoing ballistic impact. *Computational Methods in Applied Mechanics and Engineering* 2006;195:94–109.
- [29] Cook RD, Malkus DS, Plesha ME. Concepts and applications of finite element analysis New York. John Wiley & Sons; 1974.
- [30] Thomson WT. Vibration theory and applications. Englewood Cliffs, N.J.: Prentice-Hall; 1965.
- [31] Hearle JWS, Grosberg P, Backer S. Structural mechanics of fibers, yarns, and fabrics New York. Wiley-Interscience; 1969.
- [32] Chen Ming, Chen Weinong, Weerasooriya Tusit. Mechanical properties of kevlar KM2 single fiber. *Journal of Engineering Materials and Technology* 2005;127:197–203.
- [33] High performance fibers for lightweight armor. The AMPTIAC Quarterly;(2):P6, <http://amptiac.alionscience.com/quarterly>, 2005;9.
- [34] Weerasooriya T, Gunnarson CA, Moy P. Measurement of full field transient deformation on the back surface of a kevlar KM2 fabric during impact for material model validation. In: Proceeding of 11th int. Congress and Exhibition on experimental and applied mechanics, Orlando, FL; 2008, v.2, p. 992–1003.
- [35] Schiffman BA, Wetzel ED. Low velocity ballistic characterization of high performance fabrics. Internal report. Army Research Laboratory; 2006.